Phagocytosis Dynamics Depends on Target Shape

Debjani Paul,[†‡△*] Sarra Achouri,[†△] Young-Zoon Yoon,[†] Jurgen Herre,[§] Clare E. Bryant,[¶] and Pietro Cicuta[†]
[†]Cavendish Laboratory, University of Cambridge, Cambridge, United Kingdom; [‡]Department of Biosciences and Bioengineering, Indian Institute of Technology Bombay, Powai, Mumbai, India; [§]Department of Medicine and [¶]Department of Veterinary Medicine, University of Cambridge, Cambridge, United Kingdom

ABSTRACT A complete understanding of phagocytosis requires insight into both its biochemical and physical aspects. One of the ways to explore the physical mechanism of phagocytosis is to probe whether and how the target properties (e.g., size, shape, surface states, stiffness, etc.) affect their uptake. Here we report an imaging-based method to explore phagocytosis kinetics, which is compatible with real-time imaging and can be used to validate existing reports using fixed and stained cells. We measure single-event engulfment time from a large number of phagocytosis events to compare how size and shape of targets determine their engulfment. The data shows an increase in the average engulfment time for increased target size, for spherical particles. The uptake time data on nonspherical particles confirms that target shape plays a more dominant role than target size for phagocytosis: Ellipsoids with an eccentricity of 0.954 and much smaller surface areas than spheres were taken up five times more slowly than spherical targets.

INTRODUCTION

Macrophages can engulf a wide variety of targets, such as invading pathogens, dead cells, foreign airborne particles (dust and pollen), etc. Bacterial pathogens exhibit a large range of sizes, shapes, and surface features, all of which might have an effect on their virulence (1). Therefore, it is important to understand whether target properties influence their uptake. Understanding the biophysical aspects of phagocytosis will complement our biochemical understanding of the uptake process.

Phagocytosis is an actin-polymerization-dependent process for the uptake of particles larger than 0.5 μm into cells (2). Macrophages are cells forming a part of the innate immune system, and phagocytosis is central to their immune function (3). Phagocytosis is an extraordinarily complex process involving both structural rearrangement (cytoskeletal and membrane) and a complex network of signaling events. Phagocytosis plays a critical role in the clearance of infectious agents or senescent cells and is central to regulating immune responses, inflammation, and tissue remodeling (2,4). Phagocytosis also plays a role in clearing inorganic particulate material from body surfaces such as inhaled carbon or mineral particles (2). The biochemical mechanisms of phagocytosis have been extensively studied and described in the literature (2,4). The phagocytic process essentially involves three steps: recognition by receptors of either an opsonized or nonopsonized particle; receptor-mediated actin polymerization leading to internalization and cleavage of the phagosome from the cytoplasmic surface; and intracellular trafficking for phagosomal maturation. Maturation of the phagosome ultimately leads to the degradation of phagosomal contents and the induction of the appropriate immune responses.

Numerous different classes of receptors are important for particle recognition. Much is known about the opsonic receptors Fc and Complement (CR), which detect particles coated with opsonins such as antibodies or complement proteins (2,4). Less is known about the mechanisms by which phagocytosis of organisms and particles occurs in response to receptor activation by the many nonopsonic receptors. These include lectins such as Dectin-1, the mannose receptor and DEC 205, scavenger receptors such as CD36 and MARCO, Integrins, DC-SIGN, CR3, the Toll-like receptors, and CD14 (5). These are known as pattern recognition receptors because they detect recurring molecular patterns on pathogens (pathogen-associated molecular patterns) (6). Ligation of a phagocytic receptor causes clustering that activates signaling cascades, leading to actin polymerization and the extension of membrane folds that envelop the bound particle and finally fuse their leading edges to create the phagosome. Different receptors are known to generate tighter or looser phagosomes (for example, the FcR generates relatively tight phagosomes and CR3 looser phagosomes (2)). Some organisms such as *Salmonella enterica* serovar Typhimurium inject actin activators into cells to generate their own, self-customized loose phagosomal home (7). Therefore, it appears that (2,7) the nature of the particle determines the type of phagosome it will ultimately reside in by the receptors it engages.

A large number of the target parameters affecting the physical process of phagocytosis have already been identified. Here, we divide these parameters into the following three classes:

1. Geometric aspects such as size (8–11) and shape or aspect ratio (12–17);

Submitted November 6, 2012, and accepted for publication July 17, 2013.

[△]Debjani Paul and Sarra Achouri contributed equally to this article.

*Correspondence: debjani.paul@iitb.ac.in

Editor: Denis Wirtz.

0006-3495/13/09/1143/8 $2.00

http://dx.doi.org/10.1016/j.bpj.2013.07.036

2. Surface properties such as surface charge (9,18–21) and hydrophobicity (9,18,19); and
3. Mechanical aspects (22).

Target size is recognized as being a critical uptake-determining parameter. Maximum target internalization occurs in the size range of 1–3 μm (8–11). It is interesting to note that the optimum size for phagocytosis by macrophages corresponds to the size of a large number of bacteria (23). The effect of the target shape on phagocytosis was noted as early as 1957 (12), but systematic investigations at both single-particle and ensemble levels have only recently emerged. Champion and Mitragotri (13) demonstrated, for the first time to our knowledge, that the local shape of the target at the point of contact with the cell membrane determines whether phagocytosis will be initiated and the size of the target decides whether internalization will be completed. Sharma et al. (15) further probed the role of the particle shape during the binding and internalization steps of phagocytosis using polymer particles. They reported that oblate ellipsoids are internalized in preference to spheres and prolate ellipsoids. Internalization studies with inorganic particles (complexes made of cadmium telluride quantum dots and cystine), in contrast, indicated spheres were more efficiently phagocytosed than rods or needles (16). Other groups have reported that the aspect ratio of rod-like particles determines the degree of their uptake, with very high aspect ratios completely inhibiting phagocytosis (14).

The role played by the surface state of the targets (9,14,18–21) has also been studied extensively. Hydrophobic targets are much more susceptible to phagocytosis than the hydrophilic targets (9,18,19). The presence of surface charge (i.e., targets with higher net ζ-potential) also leads to increased uptake: cationic and anionic particles with comparable absolute ζ-potential values have similar levels of ingestion by macrophages (9,14,18–21). The effect of the mechanical properties of the target particle has not been explored to the same extent as particle size or surface properties. Beningo and Wang (22) studied the Fc-receptor-mediated phagocytosis of IgG-opsonized polyacrylamide beads with different stiffness values and saw that macrophages were unable to internalize soft particles. Uptake of these soft particles, however, could be artificially stimulated by adding constitutively active Rac1 or lysophosphatidic acid.

Much of the reported work into the role of target parameters in phagocytosis is limited because researchers use static, end-point outcomes of phagocytic assays and they measure the average uptake behavior of the cell population as a whole (8–12,15–22). These experiments, therefore, cannot provide information about the kinetics of the early phagocytic events, such as:

How long does each cell take to engulf a particle?
How does the engulfment time depend on the properties of the target?
Are there differences in the phagocytic capabilities of individual cells within a particular population?

To address some of these issues, a few groups are studying the cell membrane dynamics during phagocytosis (24–26). Kress et al. (26) have shown that the filopodia of macrophages retract with discrete steps (with mean step size of 36 nm). Tollis et al. (27) have distinguished between the active and the passive zipper mechanisms of phagocytosis by simulation and experiments. These authors have also reported on the effects of target size and shape on the speed of particle uptake and the completion of the phagocytic cup by imaging fixed cells at various time points.

Here we address the dependency of phagocytic uptake on target parameters by measuring the uptake times of a large number of single phagocytosis events recorded from start to finish. We monitor phagocytosed targets from their first contact with the cell membrane until internalization to determine the engulfment time for each single event. We then compare these engulfment times from a large number of single phagocytosis events to explore their dependence on target parameters. We use spherical (silica, latex, and conidia of dead fungi) and ellipsoidal (latex) beads to investigate the effect of target shape and size on the uptake time. Our main finding is that the spherical particles, which are larger than the ellipsoidal particles, are engulfed five-times faster than the ellipsoids with smaller surface areas. The data obtained using these kinetic measurements is consistent with the conclusions from existing reports (13–15,17) on the target shape dependence of phagocytosis, while quantifying the dynamics of the complete phagocytic process in live imaging at single cell level.

MATERIALS AND METHODS

Particles

Four spherical systems of different sizes and three different chemistries, silica, latex beads and dead conidia (the fungal pathogen *Aspergillus fumigatus* as representative of biological material) were chosen. These spherical phagocytosis targets were compared with ellipsoidal latex beads. Fig. 1 shows representative optical microscope images of the particles used in this study.

Uncoated silica beads of diameter 1.85 μm (Cat. No. SS04N) were bought from Bangs Laboratories, Fishers, IN. Uncoated 3-μm-diameter silica beads (Cat. No. 141211-10) were from Microspheres-Nanospheres, Corpuscular Ltd., Cold Spring, NY. Spherical carboxylated latex beads of 2-μm diameter (Cat. No. L 3780) were obtained from Sigma-Aldrich, Saint Louis, MO.

The conidia (~3 μm diameter) of *Aspergillus fumigatus* were prepared by culturing *A. fumigatus* on potato/dextrose slants (Becton Dickinson, Canaan, CT) and washing the filamentous fungal growth area vigorously with phosphate-buffered saline (PBS) (Sigma-Aldrich) to release conidia but not hyphae. Suspended conidia were collected in a dedicated tissue culture hood and washed repeatedly by centrifugation at 400*g*. The suspension of conidia was then fixed in 4% paraformaldehyde (Sigma-Aldrich) for 48 h at 4°C. The killed and fixed conidia were then repeatedly washed in PBS by centrifugation to remove paraformaldehyde and then counted. Aliquots of conidia at a concentration of 1×10^6/mL were then prepared and stored at 4°C before use.

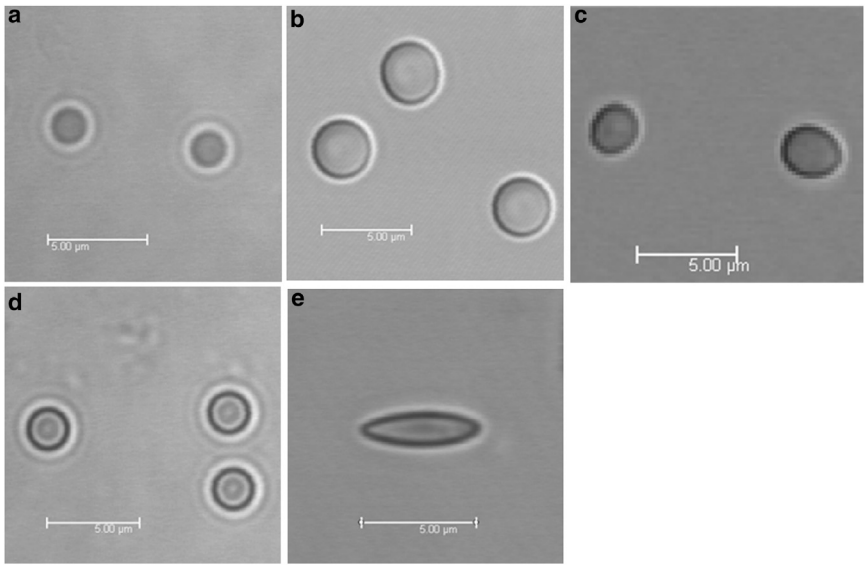

FIGURE 1 Optical micrographs of the different particles used in this study. (*a*) A 1.85-μm diameter silica sphere; (*b*) 3-μm diameter silica sphere; (*c*) ~3-μm diameter dead conidia of *Aspergillus fumigatus* (slightly ovoid); (*d*) 2-μm diameter latex sphere; and (*e*) ~1.5 × 1.5 × 5 μm latex ellipsoid. The dimensions of the ellipsoid indicate principal-axis lengths. All scale bars correspond to 5 μm.

Prolate ellipsoidal latex beads (1.5 × 1.5 × 5 μm) were a gift from Dr. Jean-Christophe Loudet, Centre de Recherche Paul Pascal, Centre National de la Recherche Scientifique, Pessac, France. Ellipsoid shapes were obtained from a previously reported procedure by Ho et al. (28).

All the particles were washed in sterile PBS solution (Sigma-Aldrich) to remove any surfactants and stored at 4°C. Before each phagocytosis assay, the beads were resuspended in complete cell culture medium and sonicated for 1–5 min to disperse them well. During imaging, 10–100 μL beads were added from the stock solution (~1 × 10^6/mL) locally onto the imaging area of the dish (i.e., around the objective) until the presence of 5–10 beads around each cell under observation could be visually confirmed.

Cell culture

The RAW 264.7 macrophage-like cell line (American Type Culture Collection, Manassas, VA) was used in all our experiments. Cells were cultured in RPMI-1640 medium supplemented with 10% fetal bovine serum (Hyclone FBS, U.S. origin; Thermo Fisher Scientific, Waltham, MA), and 2 mM L-glutamine (Sigma-Aldrich) and 10 μg/mL penicillin and streptomycin (Sigma-Aldrich).

Cells were plated on 50-mm-diameter glass-bottomed petri dishes (MatTek, Ashland, MA) (~5 × 10^5 cells per dish) 24 h before each phagocytosis assay; they were then incubated in 1–2% serum for 12–15 h, followed by at least 1 h incubation in complete (10% serum) media before imaging.

Phagocytosis assay with live cells

The phagocytosis assays were performed in a confocal microscope fitted with an imaging incubator (37°C and 5% CO_2, saturated with water vapor) to keep the macrophages healthy for the entire duration of the experiment (4–6 h). We then loaded the petri dish containing macrophages on the microscope and started image acquisition. Then, we gradually added the particles into the dish, while keeping the cells in focus. This was done to ensure that we could monitor the entire engulfment process (i.e., from the first contact with the target until phagosome formation) in real-time. We imaged at least two replicates on each day and also imaged on at least two different days when we did a phagocytosis assay with a particular target.

Time-lapse imaging

We carried out time-lapse imaging using a Leica SP5 confocal microscope (Leica Microsystems, Milton Keynes, United Kingdom). The excitation wavelength of the Ar^+ laser (kept at 20% power) was 514 nm. We acquired images through a 40× (1.25 NA) oil immersion objective in the bright-field mode. Because each phagocytosis assay lasted several hours, a software best-focus technique (using Leica contrast method 2 with 50-μm capture range and refocusing every fifth cycle) was adopted to keep the cells in focus for the entire duration of the experiment. Z-stacks at a step size of 1 μm were acquired for each time point and the time-lapse interval was chosen to be 30 s to 1 min. We manually analyzed the time-lapse images using the LAS AF LITE software (Leica Microsystems). Even though there were many phagocytosis events in our experiments, we chose only those events for data analysis that we were able to track from the first contact of the target with the cell membrane until complete internalization.

Measurement of single-event engulfment times

Fig. 2 schematically explains how single-event engulfment time was defined in our experiments. As shown in Fig. 2 *a*, we defined the start of engulfment (t_{start}) as the frame in which the target was first seen to attach irreversibly to the cell membrane. This was clear from the sudden absence of Brownian motion. The end point of engulfment (t_{end}) was defined as the frame in which

1. We could either see the formation of a complete phagosome around the bead (Fig. 2 *b*), or
2. The bead and the nucleus were in focus in the same z-frame, as illustrated by internalized ellipsoids in Fig. 2 *c*.

The engulfment time was therefore defined as $\Delta t = t_{end} - t_{start}$.

Movie S1 and Movie S2 (in the Supporting Material) show two typical phagocytosis events with silica spheres and latex ellipsoids as the respective targets. The particular target whose uptake was monitored in a frame-by-frame manner is indicated by a solid green arrow in the clips. Fig. 3 shows the images (in-focus ones) from Movie S1, with a dashed red arrow indicating the cell in question. In frames *a–c*, the cell membrane is seen to protrude towards the bead without making contact. The bead is seen to be in contact with the cell membrane for the first time in frame *d*, which is taken as the start time (t_{start}: 20 min 10 s). Frames *e–g* indicate formation

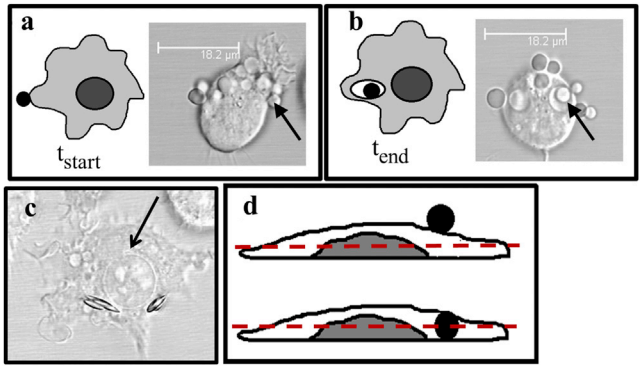

FIGURE 2 Measurement of single-event engulfment time. Start of phagocytosis (t_{start}) is schematically defined as the time point when the particle (*solid*) makes irreversible contact with the cell membrane (*a*). A silica bead (indicated by the *solid arrow*) is seen to make contact with the RAW cell membrane. Engulfment (t_{end}) is indicated either by the formation of a complete phagosome around the particle (*b*) or when the bead and the outline of the cell nucleus (shown by the *solid arrow*) are in focus in the same z-frame (*c*); ellipsoidal beads internalized by a RAW cell are seen in the panel. Z-stack imaging is used to determine whether a bead is actually ingested or is simply lying on top of the cell (*d*). The bead (*solid*) is considered to be engulfed when it lies in the same focal plane (*dashed line*) as the nucleus (*dark shaded*).

of membrane ruffles that usually accompany phagocytosis (22,23). We see the phagosome starting to form in frame *h*. A complete phagosome boundary can be seen around the bead in frame *i*, which is designated as the end time (t_{end}: 25 min 10 s). The engulfment time ($\Delta t = t_{end} - t_{start}$) for this particular event is 5 min.

Similar images from Movie S2 (uptake of a latex ellipsoid) identifying start and end times are shown in Fig. S1 (in the Supporting Material). A latex ellipsoidal particle (shown by *arrow*) is found to float freely outside the RAW cells in frame *a*. It comes in contact with the plasma membrane of one of the cells in frame *b*, which is designated as the start frame for this event. The ellipsoid remains stuck to the membrane for several minutes (frames *b*–*e*) and then gets pulled toward the inside of the cell (frame *f*). The phagosome is seen to form in frames *g*–*i*. The bead inside the complete phagosome is seen in frame *i*, which is taken as the end point of phagocytosis. The entire internalization process took ~8 min from the first contact in this case.

The attachment of the target with the cell membrane was taken to be irreversible only if the target was finally internalized. We therefore initially identified each phagocytosed target present within a cell from our time-lapse images and then went backward to identify the frame in which the particular target came in contact with the cell. We tracked each target manually from frame to frame. Start times were determined following this protocol throughout our experiments. During image acquisition, if a cell came into the field of view with the target already attached to it (i.e., if we were not able to unambiguously identify the start frame), we excluded the event from data analysis even though we could record the rest of the internalization process. As reported by other groups (13,24), we too observed formation of membrane ruffles during initiation of phagocytosis.

Sometimes the targets made temporary contact with the cell membrane, only to be released later without being taken up, as shown in Movie S3. A particle could potentially remain attached to the cell membrane for several hours without being internalized. Such a contact (i.e., one that did not lead to phagocytosis) was therefore called "reversible" and was not included in our analysis.

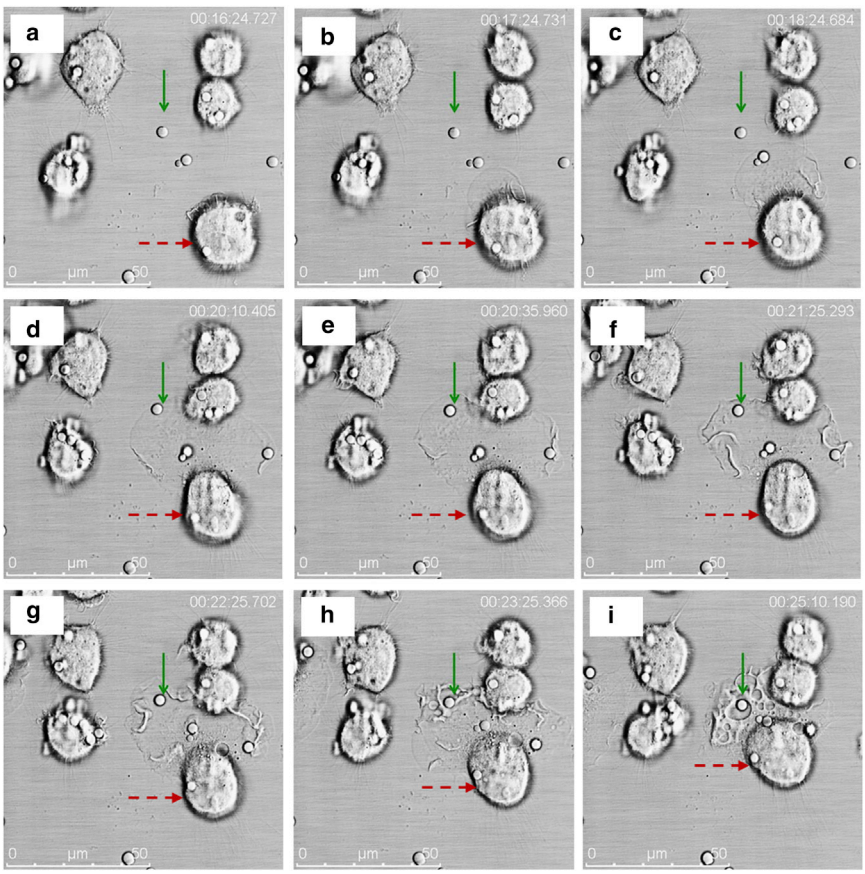

FIGURE 3 Time-lapse images from a typical phagocytosis event to illustrate the start and end points of phagocytosis. Only those frames that were in focus during z-stack data acquisition are shown here. The timestamps on the frames indicate the time elapsed since the start of image acquisition ($t = 0$). The phagocytosed bead (uncoated silica) is indicated by a solid (*green*) arrow in all the frames. The cell in question is indicated by a dashed (*red*) arrow. (*a*–*c*) The cell membrane protrudes toward the bead without making contact. (*d*) The bead is seen to be in contact with the cell membrane for the first time in this frame. Therefore, we designate this time point as the start time (t_{start}: 20 min 10 s). (*e*–*g*) Membrane ruffles usually accompanying phagocytosis are seen to form. (*h*) The phagosome starts forming, but the engulfment of the bead is not yet complete. (*i*) A complete phagosome boundary can be seen around the bead in this frame. Therefore, we call this time point as the end time (t_{end}: 25 min 10 s). The single-event engulfment time ($\Delta t = t_{end} - t_{start}$) for this particular phagocytosis event is 5 min.

In a separate experiment, we have also used optical tweezers to deliver targets to the RAW cells. Movie S4 shows a conidia being delivered by the tweezers to a cell. The spatial position of the optical trap is indicated by a red dot (also highlighted by the *arrow*). The images obtained from the tweezers experiments were very similar to the images obtained by time-lapse microscopy. We were unable to detach the conidia by pulling with the optical trap after it made irreversible contact with the filopodia and was dragged upwards by the cell (see Movie S5). This validated our observation that particle uptake is indeed occurring.

RESULTS AND DISCUSSION

Observation of phagocytosis kinetics by live imaging

The majority of the published data on phagocytosis has been obtained by fixing cells at specific time points after bead uptake and then using staining protocols to localize cellular structures. We performed instead real-time imaging combined with phagocytic event quantification, and matched our observations against the findings reported in the literature using the static imaging approaches. The steps followed in determining the start and end times of phagocytosis have been detailed in the Materials and Methods. To remove any bias from our time-lapse experiments, the responses of at least 50 cells were analyzed (imaging different parts of a dish, using multiple dishes on the same day and repeating the experiment on multiple days) for each kind of target.

Fig. 3 and Fig. S1 illustrate typical phagocytosis kinetics and the extraction of single-event engulfment times from time-lapse images. Instead of reporting the uptake rate of the cell population as a whole, we focused on extracting the kinetics from single uptake events. In our work, engulfment was measured after a target actually contacted the cell membrane. This approach has the advantage of eliminating influence of cell and target motilities on phagocytic uptake. Information similar to ours may also be obtained using optical tweezers or micropipettes (24,25) to deliver phagocytic targets. This leads, however, to additional complications because of the interaction of the laser with the cell, and biasing of the target orientation. Our approach, in contrast, allowed study of uptake kinetics under a minimal perturbation.

Inside or outside?

One of the challenges in analyzing phagocytosis data obtained by live imaging lies in clearly determining the end point of phagocytosis. Although tracking the formation of the phagosome in a frame-by-frame manner (Fig. 3 and Fig. S1) is the most unambiguous technique for determining the completion of phagocytosis, sometimes the phagosome is too tight around the particle to be clearly tracked in this way. In our experiments, therefore, the end point of phagocytosis was defined either as the frame in which a complete phagosome was seen around the target (Fig. 3 *i* and Fig. S1) or when a cell organelle, such as the nucleus, could be seen in focus along with the target while doing z-stack imaging (Fig. 2 *c*). Fig. 2 *d* schematically illustrates this last concept, with the dashed line denoting the focal plane. It is not possible to keep both the nucleus and the particle in focus if the particle is simply lying on top of the cell (*upper panel*, Fig. 2 *d*). As an example of this idea, Fig. 2 *c* shows a representative image of some ingested ellipsoidal beads. The beads are in focus along with the outline of the nucleus (shown by the *solid arrow*) in this image. When the phagosome formed around a particle that was very tight, the indirect strategy of looking for the nucleus and the bead in the same z-frame was employed.

There are several published protocols applicable in fixed cells, to distinguish internalized targets from the ones that are simply attached to the cell membrane. Typically, after fixing the cells at the end of an assay, noninternalized particles are removed by reacting with an appropriate membrane-impermeable substance such as xylene (29) or ascorbate (30). In an attempt to differentiate between the shape dependence of receptor recognition and internalization, Sharma et al. (15) allowed targets to attach to the cell membrane at 4°C (because particles cannot be ingested at this temperature) and subsequently performed internalization experiments at 37°C. More recently, Mech et al. (31) proposed an automated image analysis method to determine the position of the beads with respect to the cell membrane, without having to remove any external beads in the process. However, the requirement for fixing and staining the cells means that none of these methods are suitable for studying engulfment kinetics.

Single-event engulfment times of spherical targets depend on their size

We estimated the average single-event engulfment times for different spherical targets (silica beads of two different diameters, latex beads, and conidia) and prolate ellipsoid latex beads. We tracked several phagocytosis events from start to finish and measured the engulfment time for each event. The distribution of the engulfment times are plotted in Fig. 4. The spread in each histogram (i.e., the spread in the engulfment time data) reflects the varying phagocytic ability of the RAW cells in that particular population. Table 1 lists the average engulfment times (Δt) (mean $\pm$ standard error of mean) for each target.

The engulfment times for similar-sized (3-μm diameter) conidia and silica beads were (5.5 $\pm$ 0.6) min and (4.3 $\pm$ 0.6) min, respectively. All the 1.85-μm-diameter silica beads were engulfed in (1.5 $\pm$ 0.9) min, whereas the uptake time for 2-μm diameter latex beads came out as (3.2 $\pm$ 0.7) min, with one of the uptake events taking $>$9 min. The outlier was rejected based on Q-test (95% confidence interval) and the average engulfment time for the latex beads was (2.5 $\pm$ 0.2) min.

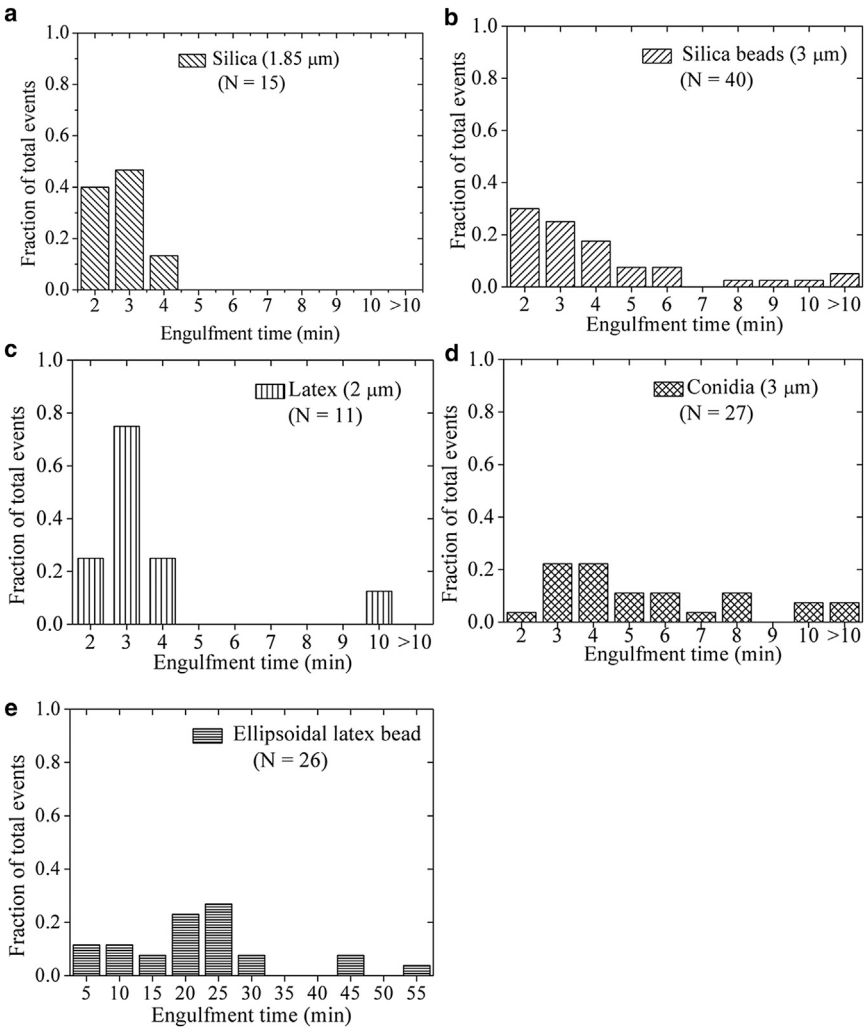

FIGURE 4 Histograms showing the distribution of engulfment time for targets of different sizes, shapes, and materials. Each plot has been normalized with respect to the total number of phagocytosis events (*N*) measured with the particular target. The spread in the distribution for each target results from the different phagocytic capabilities of the RAW cells in the particular population. (*a*) 1.85-μm silica spheres, (*b*) 3-μm silica spheres, (*c*) 2-μm latex spheres, (*d*) 3-μm conidia, and (*e*) ellipsoidal latex beads. Irrespective of size or material, >90% of the spherical targets are ingested within 10 min of making the first contact with the RAW cells, whereas only ~10% of the ellipsoids are internalized in that period.

Because the macrophage needs to cover the entire target with its cell membrane for successful engulfment, the surface area of the target can be taken to be one of the indicators of its size. As a consequence, we looked into the surface area and the engulfment time of our particles to see if any correlation exists between these two parameters. We find from Table 1 that the engulfment time increases with size for spherical particles. This is in agreement with the findings of Tollis et al. (27), who reported a similar size-dependence for passive zipper phagocytosis. Because our particles are nonopsonized and we do not expect any antibodies to be present in our heat-inactivated serum, we can attribute the observed phagocytosis events to be mediated by scavenger receptors on the RAW cells. Dectin-1-mediated uptake of conidia is not likely to be relevant in our experiments because the RAW cells express very low levels of this receptor and B-glucans (the target) are not present on the surface of conidia, only on their hyphae. Presence of large membrane ruffles during engulfment (27) leads us to classify our events as passive phagocytosis.

TABLE 1 Details of the average single-event engulfment times obtained with different targets

Target type (diameter/ principal axes)	No. of events	Average engulfment time (min)	Surface area (μm^2)
Silica sphere (1.85 μm)	15	1.5 ± 0.9	10.75
Silica sphere (3 μm)	40	4.3 ± 0.6	28.27
Conidia (3 μm)	27	5.5 ± 0.6	28.27
Latex sphere (2 μm)	11	2.5 ± 0.2	12.57
Latex ellipsoid (1.5 × 1.5 × 5 μm)	26	19.8 ± 2.4	19.12

The number of phagocytosis events analyzed and the surface areas of the targets are also listed.

Fewer phagocytosis events were observed with latex beads when compared with similar-sized silica beads. Latex beads (density ~1.05 g/cc) tend to float more in cell culture media, whereas silica beads (density ~2 g/cc) settle at the bottom of the dish more quickly, where they are easily found by the RAW cells. The floating behavior of these targets is likely to have an effect on how frequently they might come in contact with the adherent RAW cells. We start measuring engulfment only after a target has irreversibly

attached to the cell membrane; therefore, the single-event engulfment time data presented in our work is independent of any bias that may result from different collision frequencies.

Ellipsoidal targets are engulfed more slowly than spherical targets

From the data in Fig. 4 and Table 1, we found that 90% of the spherical targets (irrespective of size or material) are engulfed within 10 min of making contact with the cell, whereas only 10% of the ellipsoidal targets are engulfed during this period. All the spherical particles show very similar internalization kinetics (Δt ~1–6 min), whereas the ellipsoidal beads are engulfed almost 4–5 times slower (Δt ~20 min).

Shape of nonspherical targets, not their size, determines the single-event engulfment time

The observation that ellipsoids are engulfed more slowly than spheres led us to compare the roles of target shape and size in phagocytosis of nonspherical particles. However, there is no obvious correlation between the size and the single-event engulfment time for nonspherical particles (e.g., ellipsoids with an eccentricity of 0.954). The surface area of ellipsoids (~19 μm^2) is intermediate between those of 2-μm latex spheres (~12 μm^2) and 3-μm silica spheres (~28 μm^2). If the surface area of the particles primarily determined their uptake, then the engulfment time of ellipsoids (19.8 $\pm$ 2.4 min) would be intermediate between those of 2-μm latex (2.5 $\pm$ 0.2 min) and 3-μm (4.3 $\pm$ 0.6 min) silica beads. On the contrary, the ellipsoids are engulfed 4–5 times more slowly. We also find that 3-μm spherical silica beads are engulfed marginally faster than similar-sized but slightly ovoid conidia (aspect ratio ~1.1).

It has been shown by several groups (13,27,32,33) that the local curvature of the target at the point of contact determines the outcome of phagocytosis with nonspherical particles. The maximum number of uptake events occurs when the particles offer the highest curvature to the phagocyte (e.g., when an ellipsoid contacts the cell in an end-on manner). Although the resolution of our imaging experiments did not allow accurate determination of the initial orientation of the nonspherical targets, the wider distribution of the engulfment time histograms obtained with ellipsoidal beads and conidia possibly shows the effect of the local curvature on phagocytosis. In conclusion, our study shows that particle shape is a critical factor in determining the efficiency of phagocytosis.

CONCLUSIONS

The goal of our study was to explore the effect of target size and shape on the phagocytosis kinetics (more specifically, on single-event engulfment time) of macrophage-like RAW cells. In this particular study, we wanted to focus on the kinetics of a simple phagocytic process without opsonization. Therefore, we compared the engulfment times from a large number of single phagocytosis events obtained using various uncoated spherical targets and one ellipsoidal target.

The sizes and shapes of the particles used in our experiments are comparable to those of many common bacteria and spores. However, bacteria also have very different chemistry, leading to a variety of specific and nonspecific binding and adhesion effects (32) unlike the simple non-opsonized particles used in this work. Despite the different surface chemistry, Möller et al. (33) have very recently reported similar shape-selective phagocytic uptake of filamentous *Escherichia coli* by macrophages.

Much of the published data on phagocytosis has been obtained from experiments with fixed cells. It is now possible to match the findings from these static imaging-based studies with the results from kinetic measurements using live cells. We used a combination of z-stack and time-lapse imaging to distinguish start and end points of phagocytosis. Because this technique did not require the cells to be fixed or stained, it was compatible with experiments using live cells. We showed that the spherical particles with larger surface areas were engulfed by RAWs five-times faster than the ellipsoids with an eccentricity of 0.954. Our observations on phagocytosis kinetics confirm that both target shape and size are important uptake-determining parameters; however, target shape and curvature play a more dominant role compared to size in the engulfment kinetics.

SUPPORTING MATERIAL

One figure and five movies are available at http://www.biophysj.org/biophysj/supplemental/S0006-3495(13)00858-8.

The authors received financial support from the MRC, UK (through a Discipline Hopping Grant), EU-ITN Transpol project and Academy of Medical Sciences, UK. JH was supported by a Clinical Lectureship from the NIHR, UK. CEB acknowledges a Research Development Fellowship from BBSRC, UK. The authors would also like to thank Robert Endres and Lyndon Koens for useful discussions.

REFERENCES

1. Cabeen, M. T., and C. Jacobs-Wagner. 2005. Bacterial cell shape. *Nat. Rev. Microbiol.* 3:601–610.
2. Aderem, A., and D. M. Underhill. 1999. Mechanisms of phagocytosis in macrophages. *Annu. Rev. Immunol.* 17:593–623.
3. Burke, B., and C. E. Lewis, editors. 2002. The Macrophage. Oxford University Press, New York.
4. Underhill, D. M., and H. S. Goodridge. 2012. Information processing during phagocytosis. *Nat. Rev. Immunol.* 12:492–502.
5. Schäfer, G., M. Jacobs, …, G. D. Brown. 2009. Non-opsonic recognition of *Mycobacterium tuberculosis* by phagocytes. *J. Innate Immun.* 1:231–243.

6. Janeway, Jr., C. A., and R. Medzhitov. 2002. Innate immune recognition. *Annu. Rev. Immunol.* 20:197–216.
7. Alpuche-Aranda, C. M., E. P. Berthiaume, …, S. I. Miller. 1995. Spacious phagosome formation within mouse macrophages correlates with *Salmonella* serotype pathogenicity and host susceptibility. *Infect. Immun.* 63:4456–4462.
8. Pratten, M. K., and J. B. Lloyd. 1986. Pinocytosis and phagocytosis: the effect of size of a particulate substrate on its mode of capture by rat peritoneal macrophages cultured in vitro. *Biochim. Biophys. Acta.* 881:307–313.
9. Tabata, Y., and Y. Ikada. 1988. Effect of the size and surface charge of polymer microspheres on their phagocytosis by macrophage. *Biomaterials.* 9:356–362.
10. Koval, M., K. Preiter, …, T. H. Steinberg. 1998. Size of IgG-opsonized particles determines macrophage response during internalization. *Exp. Cell Res.* 242:265–273.
11. Champion, J. A., A. Walker, and S. Mitragotri. 2008. Role of particle size in phagocytosis of polymeric microspheres. *Pharm. Res.* 25:1815–1821.
12. Lengerova, A., V. J. Lenger, …, M. Volfova. 1957. The influence of the shape of dust particles on the rate of phagocytosis in vitro. *Br. J. Ind. Med.* 14:43–46.
13. Champion, J. A., and S. Mitragotri. 2006. Role of target geometry in phagocytosis. *Proc. Natl. Acad. Sci. USA.* 103:4930–4934.
14. Gratton, S. E. A., P. A. Ropp, …, J. M. DeSimone. 2008. The effect of particle design on cellular internalization pathways. *Proc. Natl. Acad. Sci. USA.* 105:11613–11618.
15. Sharma, G., D. T. Valenta, …, J. W. Smith. 2010. Polymer particle shape independently influences binding and internalization by macrophages. *J. Control. Release.* 147:408–412.
16. Lu, Z., Y. Qiao, …, C. M. Li. 2010. Effect of particle shape on phagocytosis of CdTe quantum dot-cystine composites. *MedChemComm.* 1:84–86.
17. Champion, J. A., and S. Mitragotri. 2009. Shape induced inhibition of phagocytosis of polymer particles. *Pharm. Res.* 26:244–249.
18. Ahsan, F., I. P. Rivas, …, A. I. Torres Suarez. 2002. Targeting to macrophages: role of physicochemical properties of particulate carriers—liposomes and microspheres—on the phagocytosis by macrophages. *J. Control. Release.* 79:29–40.
19. Faraasen, S., J. Vörös, …, E. Walter. 2003. Ligand-specific targeting of microspheres to phagocytes by surface modification with poly(L-lysine)-grafted poly(ethylene glycol) conjugate. *Pharm. Res.* 20:237–246.
20. Roser, M., D. Fischer, and T. Kissel. 1998. Surface-modified biodegradable albumin nano- and microspheres. II: Effect of surface charges on in vitro phagocytosis and biodistribution in rats. *Eur. J. Pharm. Biopharm.* 46:255–263.
21. Gilberti, R. M., G. N. Joshi, and D. A. Knecht. 2008. The phagocytosis of crystalline silica particles by macrophages. *Am. J. Respir. Cell Mol. Biol.* 39:619–627.
22. Beningo, K. A., and Y.-L. Wang. 2002. Fc-receptor-mediated phagocytosis is regulated by mechanical properties of the target. *J. Cell Sci.* 115:849–856.
23. Kubitschek, H. E. 1969. Growth during the bacterial cell cycle: analysis of cell size distribution. *Biophys. J.* 9:792–809.
24. Coelho Neto, J., U. Agero, …, O. N. Mesquita. 2005. Real-time measurements of membrane surface dynamics on macrophages and the phagocytosis of *Leishmania* parasites. *Exp. Cell Res.* 303:207–217.
25. Lee, C.-Y., M. Herant, and V. Heinrich. 2011. Target-specific mechanics of phagocytosis: protrusive neutrophil response to zymosan differs from the uptake of antibody-tagged pathogens. *J. Cell Sci.* 124:1106–1114.
26. Kress, H., E. H. K. Stelzer, …, A. Rohrbach. 2007. Filopodia act as phagocytic tentacles and pull with discrete steps and a load-dependent velocity. *Proc. Natl. Acad. Sci. USA*. 104:11633–11638.
27. Tollis, S., A. E. Dart, …, R. G. Endres. 2010. The zipper mechanism in phagocytosis: energetic requirements and variability in phagocytic cup shape. *BMC Syst. Biol.* 4:149.
28. Ho, C. C., A. Keller, …, R. H. Ottewill. 1993. Preparation of monodisperse ellipsoidal polystyrene particles. *Colloid Polym. Sci.* 271: 469–479.
29. Gardner, D. E., J. A. Graham, …, D. L. Coffin. 1973. Technique for differentiating particles that are cell-associated or ingested by macrophages. *Appl. Microbiol.* 25:471–475.
30. Ito, T., M. J. Ueda, …, S.-I. Ohnishi. 1981. Phagocytosis by macrophages. II. The dissociation of the attachment and ingestion steps. *J. Cell Sci.* 51:189–201.
31. Mech, F., A. Thywissen, …, M. T. Figge. 2011. Automated image analysis of the host-pathogen interaction between phagocytes and *Aspergillus fumigatus*. *PLoS ONE.* 6:e19591.
32. Gog, J. R., A. Murcia, …, C. E. Bryant. 2012. Dynamics of *Salmonella* infection of macrophages at the single cell level. *J. Roy. Soc. Interface.* 9:2696.
33. Möller, J., T. Luehmann, …, V. Vogel. 2012. The race to the pole: how high-aspect ratio shape and heterogeneous environments limit phagocytosis of filamentous *Escherichia coli* bacteria by macrophages. *Nano Lett.* 12:2901–2905.